



UNIVERSITY OF GOTHENBURG

Gothenburg University Publications

Formation of oxidized phosphatidylinositol and 12-oxo-phytodienoic acid containing acylated phosphatidylglycerol during the hypersensitive response in Arabidopsis

This is an author produced version of a paper published in:

Phytochemistry (ISSN: 0031-9422)

Citation for the published paper:

Nilsson, A. ; Johansson, O. ; Fahlberg, P. (2014) "Formation of oxidized phosphatidylinositol and 12-oxo-phytodienoic acid containing acylated phosphatidylglycerol during the hypersensitive response in Arabidopsis". *Phytochemistry*, vol. 101 pp. 65-75.

<http://dx.doi.org/10.1016/j.phytochem.2014.01.020>

Downloaded from: <http://gup.ub.gu.se/publication/205314>

Notice: This paper has been peer reviewed but does not include the final publisher proof-corrections or pagination. When citing this work, please refer to the original publication.

Formation of oxidized phosphatidylinositol and 12-oxo-phytodienoic acid containing acylated phosphatidylglycerol during the hypersensitive response in Arabidopsis

Anders K. Nilsson, Oskar N. Johansson, Per Fahlberg, Feray Steinhart, Mikael B. Gustavsson, Mats Ellerström, and Mats X. Andersson *

Department of Biological- and Environmental Sciences, University of Gothenburg, Box 461, SE-405 30 Göteborg

Correspondence to:

Mats X. Andersson

Department of Biological and Environmental sciences, University of Gothenburg

Box 461

SE-405 30 Göteborg

Sweden

Email: mats.andersson@bioenv.gu.se

Phone: +46 31 786 2688

Abstract

Plant membranes are composed of a wide array of polar lipids. The functionality of these extends far beyond a pure structural role. Membrane lipids function as enzyme co-factors, establish organelle identity and as substrates for enzymes such as lipases and lipoxygenases. Enzymatic degradation or oxidation (enzymatic or non-enzymatic) of membrane lipids leads to the formation of a diverse group of bioactive compounds. Plant defense reactions provoked by pathogenic microorganisms are often associated with substantial modifications of the lipidome. In this study, we profiled changes in phospholipids during the hypersensitive response triggered by recognition of the bacterial effector protein AvrRpm1 in *Arabidopsis thaliana*. A simple and robust LC-MS based method for profiling plant lipids was designed to separate all the major species of glycerolipids extracted from Arabidopsis leaf tissue. The method efficiently separated several isobaric and near isobaric lipid species, which otherwise are difficult to quantify in direct infusion based profiling. In addition to the previously reported OPDA-containing galactolipids found to be induced during hypersensitive response in Arabidopsis, three OPDA-containing sulfoquinovosyl diacylglycerol species, one phosphatidylinositol species as well as two acylated OPDA-containing phosphatidylglycerol species were found to accumulate during the hypersensitive response in Arabidopsis. Our study confirms and extends on the notion that the hypersensitive response in Arabidopsis triggers a unique profile of Allene Oxide Synthase dependent oxidation of membrane lipids. Primary targets of this oxidation, seems to be uncharged and anionic lipid species.

Keywords:

Membrane lipid, arabidopside, hypersensitive response, 12-oxo-phytodienoic acid, lipid profiling, galactolipid

1. Introduction

Plant cellular and organellar membranes are composed of a large and diverse array of polar lipids. Apart from their obvious structural role, they also serve as precursors for signaling compounds and regulators of many different cellular processes (Wang, 2004). Phospholipase C (PLC) and D (PLD) which cleaves off the headgroup of glycerophospholipids leaving diacylglycerol (DAG) or phosphatidic acid (PA), respectively, are involved in intracellular signaling. In plants, PLC and PLD activity are linked to various biotic and abiotic stress responses (Li et al., 2009; Testerink and Munnik, 2011; Wang, 2004). Plant membrane lipids are rich in polyunsaturated fatty acids susceptible to oxidation by enzymatic or non-enzymatic processes. The oxidation of polyunsaturated fatty acids gives rise to a plethora of oxidized products collectively known as oxylipins (Andreou et al., 2009), among these the best understood are the members of the jasmonate family of plant hormones (Browse, 2009; Gfeller et al., 2010; Schaller and Stintzi, 2009). The oxylipins constitute both free fatty acids or fatty acid fragments and glycerolipid bound acyl groups. Generally, the role of oxylipins esterified to complex lipids is much less understood than that of the free fatty acids and fatty acid fragments. Among the lipid bound oxylipins are the so called arabidopsides which are chloroplast galactolipids containing enzymatically formed 12-oxo-phytodienoic acid (OPDA) and/or the C16 analogue dinor-OPDA (Andersson et al., 2006a; Buseman et al., 2006; Hisamatsu et al., 2003; Hisamatsu et al., 2005; Kourtchenko et al., 2007).

Plants recognize and defend themselves against phytopathogenic microorganisms by a complex layered system (Jones and Dangl, 2006). A first layer is based on the ability to recognize typical microbial molecular structures known as Microbe Associated Molecular Patterns (MAMPs) (Monaghan and Zipfel, 2012). Plant pathogens have adapted to overcome the defense mounted after MAMP recognition. To this end the pathogens use secreted proteins known as effectors (Bent and Mackey, 2007). However, plants have in turn developed systems for recognition of the pathogenic effectors by so called R proteins. Recognition of pathogenic effectors often leads to a strong resistance response that frequently culminates in the so called hypersensitive response (HR) and programmed cell death. Previous studies indicate the involvement of phospholipases C (PLC) and D (PLD) in both MAMP and effector triggered responses (Andersson et al., 2006b; Kirik and Mudgett, 2009; Pinosa et al., 2013; van der Luit et al., 2000; Wang, 2004). Production of various oxylipins has also been reported in conjunction with primarily the HR (Andersson et al., 2006a; Kourtchenko et al., 2007; Montillet et al., 2005; Rusterucci et al., 1999; Vu et al., 2012; Zoeller et al., 2012). We have previously reported that PLD and PLC are involved in signaling triggered after recognition of the *Pseudomonas syringae* effector AvrRpm1 by the R-protein RPM1 and the effector R-protein pair AvrRpt2 and RPS2 (Andersson et al., 2006b). In addition, (dn)OPDA-containing galactolipids have

been shown to accumulate in Arabidopsis tissue undergoing the HR (Andersson et al., 2006a; Kourtchenko et al., 2007; Vu et al., 2012; Zoeller et al., 2012). These are probably formed by the direct Lipoxygenase 2 (LOX2) and Allene Oxide Synthase (AOS) dependent oxidation and cyclisation of 16:3 and 18:3 bound to galactolipids (Glauer et al., 2009; Nilsson et al., 2012). Several other types of lipid bound oxidized and fragmented fatty acids were shown to accumulate in Arabidopsis tissue following the HR induced by *P. syringae* expressing AvrRpm1 (Zoeller et al., 2012).

There are several approaches available to profile complex lipids from plant tissue. Classically, complex lipids are separated into lipid classes by straight phase chromatography (HPLC or TLC) before hydrolysis and analysis of the liberated fatty acids by GC or HPLC. This quickly becomes cumbersome and it is usually not possible to entirely reconstruct the species composition of the lipid classes. Modern approaches to lipid profiling utilize tandem mass spectrometry, where specific scan modes are used to detect different lipid classes using head group specific fragmentation. A total lipid extract can be directly injected into the electrospray ion (ESI) source of a triple quadrupole mass spectrometer and using head group specific scans to construct a total lipid profile (Brügger et al., 1997; Isaac et al., 2007; Taguchi et al., 2005; Welti et al., 2003). This approach is highly efficient and has facilitated large advances in plant lipid research. However, direct infusion into the mass spectrometer comes with certain limitations. A complex mixture causes ion suppression in the source which has to be accounted for by the use of multiple internal standards. The common plant lipid molecular species are separated by only one or two unsaturations, which require isotopic deconvolution. Moreover, many lipid species are nearly or truly isobaric and thus impossible or difficult to separate in direct infusion experiments. Coupling mass spectrometry to online separation by HPLC alleviates many of these problems and several systems for both reverse and straight phase separation of membrane lipids have been described (see for example (Ibrahim et al., 2011; Laaksonen et al., 2006; Okazaki et al., 2013; Retra et al., 2008)).

In this study we developed a simple and robust method using ESI-MS coupled to reverse phase HPLC for profiling plant glycerolipids. The method was used to investigate AOS dependent changes in cellular phospholipids during the HR induced by the bacterial effector AvrRpm1. This led to the identification of unexpected oxidized derivatives of phosphatidylglycerol (PG) and phosphatidylinositol (PI).

2. Results

2.1. Development of a LC-MS method for profiling plant glycerolipids

We intended to extend our previously used galactolipid separation method (Kourtchenko et al., 2007; Nilsson et al., 2012) to a wider range of glycerolipids and use tandem mass spectrometry to profile membrane lipids during the HR in Arabidopsis tissue. To this end we used head group specific multiple reaction monitoring (MRM) for the major Arabidopsis glycerolipids (Isaac et al., 2007) and the major acylated MGDG species in Arabidopsis (Ibrahim et al., 2011) (Table 1). A gradient system previously used for galactolipids (Nilsson et al., 2012) initially seemed promising for separation of phospholipids as well. However, in our hands C18-columns never provided satisfactory separation of phosphatidylcholine (PC) species using the solvent system composed of acetonitrile:water and 2-propanol, whereas a C8 column gave sharp symmetric peaks of PC species. Change to a C8 column shortened the retention and thus an initial solvent mixture with a higher water content of the initial mobile phase was required to obtain good separation of OPDA-containing MGDG species. A gradient from Solvent A (acetonitrile:methanol:water, 35:35:30 by vol.) to 2-propanol was used. To facilitate ionization, both solvents were supplemented with formic acid and ammonia. We next aimed to obtain good separation of phosphatidic acid (PA) species. Initially, chromatographic performance of this lipid was poor. An excess of formic acid and addition of a low concentration (5 μ M) of phosphoric acid to the solvent as described (Ogiso et al., 2008) gave fully satisfactory separation of PA. Taken together, this provided good separation of all major known species of PC (Fig. 1A), phosphatidylethanolamine (PE, Fig. 1B), phosphatidylglycerol (PG, Fig. 1C), PA (Fig. 1D), lyso-PC (Fig. 1E), monogalactosyldiacylglycerol (MGDG, Fig. 1F), digalactosyldiacylglycerol (DGDG, Fig. 1G) sulfoquinovosyl diacylglycerol (SQDG, Fig. 1H), OPDA-containing MGDG species (Arabidopsides A-D and MGDG-O, Fig. 1I) and acylated monogalactosyldiacylglycerol species (Fig. 1J). Interestingly, lyso-PC species separated into two distinct peaks for each fatty acid-head group combination (Fig 1E). We interpret this as separation of the *sn*-1 and *sn*-2 lyso isomers (Adlercreutz and Wehtje, 2001; Creer and Gross, 1985). For most lipid classes, each mass transition corresponded to a single major peak. A secondary peak could often be ascribed to isotopic peaks of the next more saturated lipid species. However, in some notable cases there was clear separation of isobaric species. The PG species corresponding to 34:3 and 34:4 split into two well separated peaks each (Fig. 1C). Product spectra in negative mode of the corresponding deprotonated PG-species showed that the first eluting peak in both pairs corresponded to a lipid species containing 16:0 whereas the second contained 16:1.

2.2. Profiling phospholipids during the HR in Arabidopsis tissue

Specific mass transitions as used above are suitable to obtain quantitative data for known compounds. We intended to investigate if the method was suitable for *de novo* discovery of phospholipid species as well. Lipids obtained from transgenic Arabidopsis leaf tissue expressing the *Pseudomonas syringae* effector AvrRpm1 driven by a DEX inducible promoter were analyzed

(Andersson et al., 2006a; Andersson et al., 2006b). Since several lipids that are dependent on the jasmonate synthesis pathway are known to accumulate during the HR (Andersson et al., 2006a; Vu et al., 2012; Zoeller et al., 2012), we also included a line with the DEX inducible AvrRpm1 construct in the *delayed-dehiscence2-2* (*dde2-2*) mutant background. The *dde2-2* mutation causes a frameshift in the gene encoding AOS (von Malek et al., 2002) and is thus unable to synthesize (dn)OPDA, jasmonates and (dn)OPDA-containing galactolipids. As a control, a line expressing AvrRpm1 in the *rpm1-3* mutant background was used. The *rpm1-3* mutant is a protein null for the R-protein RPM1 and thus unable to recognize AvrRpm1 (Grant et al., 1995). To test and compare the HR between the three different lines, leaf explants were incubated in water with DEX and the amount of released cellular electrolytes was measured with a conductivity electrode. As previously reported, expression of AvrRpm1 in the Col-0 background led to a large increase in electrolyte leakage with maximum increase at about 2 h after induction and at 6 hours an essentially complete release (Andersson et al., 2006b) (Fig 2A). The HR as measured by release of electrolytes did not differ in the Col-0 and *dde2-2* mutant backgrounds. We also measured the fresh and dry weight at 0, 6 and 24 h after DEX addition (Fig 2B). This demonstrated a decrease in both fresh and dry weight of the leaf explants from DEX:AvrRpm1/Col-0 and DEX:AvrRpm1/*dde2-2* of about 20-30%. Leaf discs from the three different lines were incubated with DEX for 6 hours and a phospholipid fraction was extracted. The obtained lipid fraction was subjected to separation with the mass spectrometer in full scan mode from m/z 400-1200. The data was exported and analyzed in MZmine2 (Pluskal et al., 2010). An example 2D plot of m/z against retention time for phospholipids in negative ionization mode is shown in figure 3A. Peaks were identified in all chromatograms using automated peak picking in MZmine2. This resulted in a list of 160 distinct peaks in the combined chromatograms of the three genetic backgrounds extracted at zero time or 6 hours after induction of AvrRpm1 expression.

The peak areas for the 160 peaks were integrated and combined for all 12 samples (two replicates, two time points and three lines) and used for correspondence analysis in order to create a two-dimensional ordination of the samples (Fig. 3B). The method gives a graphical representation of the likeness of samples, with increasing distance representing decreasing similarity. This clearly shows a very close grouping of the replicate samples and that recognition of AvrRpm1 has a profound effect on the phospholipid profile. In addition, the absence of functional AOS clearly provided yet another large qualitative shift in the overall lipid profile. It appears as if the recognition of AvrRpm1 causes shift along one coordinate and the AOS dependent change provides shift in the other coordinate.

To extract phospholipid peaks from the data set that were strongly induced by the recognition of AvrRpm1, the peak list was sorted for statistical significance (Student's *t*-test, $p < 0.05$) between the 6 hour samples of DEX:AvrRpm1/Col-0 and DEX:AvrRpm1/*rpm1-3*, and a minimum of three times

larger average peak area in DEX:AvrRpm1/Col-0. This resulted in a total of 14 distinct peaks which were further split in two groups: one corresponding to those not affected by the *dde2-2* mutation (AOS-independent) and one corresponding to those not induced in the *dde2-2* background (AOS-dependent, Table 2, 1-6 and 7-14, respectively).

The induction of the identified compounds during the HR was confirmed in a replicate run using independent samples and single ion monitoring for the 14 identified peaks (Fig. 4A and B). Clearly, several of the AOS-independent peaks were more strongly induced in the *dde2-2* background than in wild type background (Fig. 4A). However, the level of induction was generally very high for the AOS dependent peaks (Fig. 4B). The sum of species for (as indicated in Table S1) PC, PG, PE, MGDG, DGDG, PA, OPDA-containing MGDG and DGDG species and OPDA- and normal fatty acid containing acylated MGDGs was calculated and normalized to DEX:AvrRpm1/Col-0 at zero time. (Fig. 5) There was a clear induction of PA after recognition of AvrRpm1, which was independent of AOS (Fig. 5A). Furthermore, the OPDA-containing MGDG and DGDG species as well as acylated MGDGs were induced after recognition of AvrRpm1 (Fig. 5B). Non oxidized acylated MGDG was approximately twice as induced in the *dde2-2* background as in the wild type background. MGDG, DGDG, PC, PE and PG were all reduced in content after recognition of AvrRpm1. However, reduction was quite moderate at 2 hours reaching about 50% after 6 hours. As expected all the Arabidopsides were absent from material obtained from DEX:AvrRpm1/*dde2-2*.

2.3. Identification of AOS-dependent and AOS-independent phospholipids induced during the HR

Product scans of the peaks identified in table 2 were used to obtain initial preliminary identities of the lipids (Table 3). This was successful for 1, 6 and 7-14. However, four of the AOS independent peaks were difficult to fragment and the limited amount of sample did not permit a systematic exploration of collision energies and other settings. These compounds also appeared to be somewhat unstable and hard to purify. We thus did not pursue peaks 2-6 any further. Peak 1 was consistent with a phosphatidylinositol (PI) carrying 16:0 and a hydroxylated 18:3 fatty acid as described previously (Zoeller et al., 2012). The identity was supported by acyl specific anions for 18:3-OH and 16:0 as well as the head group specific fragment of m/z 241.5. Furthermore, positive mode fragments of the corresponding protonated ion produced a fragment consistent with diacylglycerol 34:3-0. Peak 6 could be established as 18:2, 18:3-PA. This was confirmed by PA-specific MRMs (see further section 2.1) and co-chromatography with an authentic standard.

Peaks 7-10 produced prominent fragments indicative of OPDA or another 18:3-derived ketol and 16:0 or 16:1. Peaks 9 and 10 thus likely represent the OPDA-containing thylakoid PG species as previously reported (Buseman et al., 2006). Compounds 7 and 8 produced similar anions as 9 and 10 and the mass of the mother anion would be consistent with PG species containing 16:0 or 16:1, OPDA and a third OPDA esterified to the head group. In agreement with this notion, the protonated adducts of B1-B4 produced DAG fragments consistent with 34:4-0 (7 and 9) or 34:3-O (8 and 10). To further establish the structures of the lipids corresponding to peaks 7 and 8, the compounds were purified from a large scale extraction of DEX:AvrRpm1/Col-0 material. GC-MS analysis of fatty acid methyl esters of the purified B1 and B2 fractions confirmed the presence of 16:1 Δ 3-trans and OPDA in 7, and 16:0 and OPDA in 8. This also pointed to an approximate stoichiometry of 2:1 for OPDA and the C16 fatty acid. This thus supports the tentative structures shown in figure 6.

Negative mode product ion spectra of compounds 11, 13 and 14 were all consistent with SQDG species containing OPDA or possibly another C18 keto fatty acid. There were clear ions of the acyl fragments in addition to a strong fragment corresponding to the sulfoquinovosyl head group (m/z 225) (Gage et al., 1992; Welti et al., 2003). Thus, ordinary acetone elution from a silica column does clearly not completely elute oxidized SQDG-species. Compound 12 yielded acyl fragments consistent with 16:0 and OPDA or a C18:3 keto fatty acid and the PI specific head group fragment m/z 241.5. The positive mode fragmentation also yielded a major fragment consistent with 34:4-O-DAG.

Fractions corresponding to peaks 1 and 7-14 were collected manually and directly injected into the source of a QTOF mass spectrometer operated in negative mode to obtain exact masses (Table 3). The measured masses were identical to the theoretical masses up to three decimals, supporting the identities of the lipid species.

Positive mode fragmentation of the MH^+ adducts of 1 and 12 demonstrated prominent neutral loss of m/z 260, a transition indicative of loss of inositolphosphate (Cole and Enke, 1991). This led us to analyze lipids from the transgenic lines using neutral loss scanning for PI (Fig. 7A). At zero time in DEX:AvrRpm1/Col-0 the two major peaks represented 34:2- and 34:3-PI, as expected (Welti et al., 2002). Six hours after induction of AvrRpm1 transcription there was a strong decrease in these two peaks concomitant with the induction of two earlier eluting species. The latter two correspond to compounds 1 and 12 and represent PI species carrying 16:0 and an oxygenated C18, B6, likely OPDA or another C18 keto fatty acid. Peak 1 thus likely represent PI carrying a 16:0 and an 18:3-OH fatty acid. Both 1 and 12 were strongly induced already at two hours in the Col-0 background, whereas there was no induction of either peak in the *rpm1-3* background (Fig 4 and 7B). Finally, compound 12 was not found in the *dde2-2* background (Table 2 and Fig 4B and 7).

3. Discussion and Conclusions

We herein report a simple reverse phase LC-MS method for the separation of plant glycerolipids. We could successfully separate lipid species of all major known polar glycerolipid classes in Arabidopsis leaf tissue. While direct infusion methods have been extremely successful in many lipidomic studies, they come with certain limitations. Ion suppression in the ion source and the very large prevalence of isobaric and near isobaric species in the plant lipidome limits the applicability. For instance, the abundant MGDG species containing two 18:3 fatty acids (monoisotopic molecular weight 774.62) is nearly isobaric to MGDG esterified with OPDA and dnOPDA (Arabidopside A, monoisotopic molecular weight 774.55). While these two are separable by a high resolution instrument, they are not separable by more standard (and generally more affordable) quadrupole instruments. Other combinations of fatty acids are truly isobaric and thus not separable in a direct infusion experiment using the common head group specific scan modes. This can be overcome by the use of acyl specific scan modes. Furthermore, diacyl lipids might fragment in the ion source to give rise to lyso-lipids and these cannot be separated from true lyso-lipids present in the extract. Coupling HPLC separation to the mass spectrometry alleviates many of these problems and several systems have been described. We adapted a previously used binary gradient (Nilsson et al., 2012) and optimized it to a C8 column to allow the analysis of the Arabidopsis lipidome.

Using only the head group specific transition described previously (Brügger et al., 1997; Ibrahim et al., 2011; Samarakoon et al., 2012; Welti et al., 2003), we could clearly distinguish several isobaric and near isobaric plant lipid species. For instance, two different isobaric pairs of PG species corresponding to 34:3 and 34:2, one carrying 16:1 and the other 16:0, could be separated (Fig. 1C). Several oxidized lipids, such as the OPDA-containing galactolipids, are near isobaric to non-oxidized lipids. Since the oxidized fatty acids cause a marked shift towards higher polarity these are easily distinguished in the reverse phase method (Fig 1F, I and J). The identification of these lipids would otherwise require high resolution instrument or acyl specific scans. The method has not yet been thoroughly evaluated for other lipid classes than those reported herein, but preliminary data suggests that triacylglycerols, sterol glycosides, glycosyl-cerebrosides as well as sulfonate containing lipids isolated from marine copepods also separate and ionize well in the same system.

The ability to use the system for a non-targeted screen for phospholipids was tested using lipid extracts from Arabidopsis leaves undergoing the HR after recognition of the *P. syringae* derived effector protein AvrRpm1. Previous studies have shown that effector triggered HR in Arabidopsis results in accumulation of PA through the activation of PLD and PLC (Andersson et al., 2006b; Kirik

and Mudgett, 2009; Zhao et al., 2013) as well as accumulation of OPDA-containing galactolipids (Andersson et al., 2006a; Kourtchenko et al., 2007; Vu et al., 2012; Zoeller et al., 2012). Clearly, we could distinguish overall changes in phospholipid profile induced during the HR. Furthermore, a short list of strongly HR induced phospholipid species could be derived from the profiling experiment. Tentative identities could be assigned to 10 of the 14 peaks induced lipids using product ion scans. The presence of OPDA rather than any other 18:3-ketol was confirmed for two compounds after purification. The putative structures were supported by accurate mass spectrometry. The 10 lipid species could be identified as one PA species, two OPDA-containing PG species, three OPDA-containing SQDG species, two oxidized PI species and two acylated-OPDA containing PG species. The lipids identified as putative OPDA-containing lipids were clearly dependent on a functional AOS enzyme as none of these accumulated in response to the HR in the *dde2-2* mutant background.

Targeted lipid analysis confirmed previous findings that PA and Arabidopsides are induced during the HR (Andersson et al., 2006a; Andersson et al., 2006b; Kirik and Mudgett, 2009; Kourtchenko et al., 2007; Vu et al., 2012). We also report that major acylated MGDG species containing only the “normal” non-oxidized fatty acids described by Ibrahim et al. (Ibrahim et al., 2011) were induced during the HR in addition to the acylated Arabidopsides. In the absence of AOS, there was a stronger induction of non-oxidized acylated MGDG. This thus supports the previous notion that wounding or, in this case, the HR first triggers the quick LOX2 and AOS dependent conversion of lipid bound 18:3 and 16:3 in the thylakoid membrane to OPDA and dnOPDA, respectively, and that this is then followed by the slower transfer of acyl groups from the glycerol backbone of galactolipids to the head group of other galactolipids (Nilsson et al., 2012). Furthermore, in the absence of lipid dependent formation of OPDA-containing MGDG, the HR still results in formation of acylated MGDG species. The thylakoid MGDG is thus apparently still acylated following induction of the HR in the absence of AOS-dependent formation of lipid bound (dn)OPDA.

Oxidized SQDG species have previously been identified in lipid extracts from wounded Arabidopsis leaf tissue (Ibrahim et al., 2011). However, the three AOS-dependent, likely OPDA-containing, SQDG species described here were not previously reported. A likely reason for this is that the OPDA-containing SQDG species are too polar to elute in the classical glycolipid fraction in acetone from a silica column. Two OPDA-containing PG species have previously been reported to accumulate after wounding and during HR induced by avirulent *P. syringae* in Arabidopsis (Buseman et al., 2006; Vu et al., 2012). Both these PG species were strongly induced also in response to the recognition of AvrRpm1 in an AOS-dependent fashion. Furthermore, to the formation of OPDA-containing PG species can now be added acylated OPDA-containing PG (Fig. 6). Uncertainties to the structures remain as it cannot from mass spectrometry alone be determined where on the glycerol backbone

and the headgroup glycerol the different fatty acids are attached. However, given the normal species composition of thylakoid PG (Dorne and Heinz, 1989), it is likely that the lipids contain 16:0 or 16:1 attached to the *sn*-2 position, OPDA at *sn*-1, and a second OPDA at one of the two positions on the glycerol moiety of the head group. Acylated PG has previously been reported to occur in oat seeds (Holmback et al., 2001). In this case, the third fatty acid was strictly associated to one of the hydroxyl groups on the head group of PG. Thus, the tentative structure shown in figure 6 is based on these previous reports on the positions of the fatty acids. These molecules are structurally similar to OPDA-containing acylated galactolipids. We suggest that the OPDA-containing acylated PG species reported herein are formed in the same way as proposed for Arabidopside E and G; thylakoid PG is enzymatically oxidized to OPDA-containing PG and then a second OPDA moiety is transferred from the backbone of a donor lipid to the head group of a PG molecule. It cannot be proven at this point, but it seems likely that this enzyme is the same as the enzyme generating acylated galactolipids upon wounding and HR.

The combined results of this and other studies (Andersson et al., 2006a; Kourtchenko et al., 2007; Vu et al., 2012; Zoeller et al., 2012) show that the lipid classes MGDG, DGDG, PG, SQDG and PI represent targets for enzymatic conversion into OPDA-containing lipids during the HR. This is consistent with the plastid localization of the LOX2 and AOS. In this view, the very prominent AOS dependent production of OPDA- and/or C18 keto-containing PI during the HR is quite unexpected. PI carrying colneleic acid has previously been reported to occur in potato tubers (Fauconnier et al., 2003) and thus PI is known to be associated with enzymatically oxidized fatty acids. PI is found only in very low concentrations in the thylakoid membrane and there is no consensus on whether or not PI is a *bona fide* thylakoid lipid or not (Moreau et al., 1998). There is PI present in the envelope membranes of chloroplasts, but overall, PI is considered to be a mainly extraplastidial lipid. Two different scenarios might explain this. Firstly, the chloroplasts might become leaky or disintegrate during the HR and thereby release the necessary enzymes for accessing the PI pool. Alternatively, PI is somehow trafficked to the chloroplasts. If the first hypothesis is true, there has to be an explanation for why only PI and not the more abundant lipid classes PE and PC become oxidized in the same fashion. On the other hand, the alternative; trafficking of PI to the chloroplast, would require yet unknown pathways. One simple explanation could be that PI, SQDG and PG all are anionic and MGDG and DGDG are uncharged, whereas PC and PE are zwitterionic. Little is known about the requirements for how LOX2 and AOS accept lipid bound fatty acids, but it would certainly be interesting to test if the enzymes are restricted to uncharged and anionic lipids.

All the “normal” membrane lipids analyzed decreased in the leaf tissue following recognition of AvrRpm1. This is in contrast to recent report of large increases in several membrane and storage lipid

species following infiltration of leaves with *P. syringae* expressing AvrRpm1 (Zoeller et al., 2012). We cannot at this point explain this discrepancy. However, three different not mutually exclusive explanations may be put forward. Firstly, responses triggered by bacterial MAMPs and other effectors are not activated in the DEX:AvrRpm1 transgenic system. Secondly, in this study leaf explants were incubated in water for a maximum of 6 hours as compared to leaves attached to the plant for 24 hours. Finally, a constant number of leaf discs for each sample were used in this study rather than normalization to tissue dry weight. If the HR leads to a substantial decrease in dry weight, it might explain at least part of the difference. We found that the HR indeed leads to a certain loss of dry weight and this might thus partially explain the difference. However, the dry weight change found cannot fully compensate for the reported increase in lipid content.

It has become abundantly clear that Arabidopsis induces a specific pathway of membrane lipid oxidation during the HR. This leads to large scale accumulation of MGDG, DGDG, SQDG, PG and PI lipid species containing (dn)OPDA. Some of these, mainly MGDG and PG, are thereafter further re-arranged to acylated (dn)OPDA-containing species. The function of the (dn)OPDA-containing lipids remains uncertain. Nevertheless, the sheer amounts formed do imply some kind of role in defense. On the other hand, the HR associated programmed cell death is apparently not significantly affected by the loss of AOS and, likewise, defense against *P. syringae* expressing effectors is not strongly affected in the *dde2-2* mutant (Sato et al., 2010; Tsuda et al., 2009). It has been suggested that OPDA-containing galactolipids might act as chemical defensive compounds against insects and microorganisms as well as function for delayed release of OPDA (Andersson et al., 2006a; Glauser et al., 2009; Kourtchenko et al., 2007).

To conclude, we herein present a simple LC-MS method for profiling plant glycerolipids and used this to identify two novel OPDA-containing acylated PG species, one likely OPDA-containing PI species and several OPDA-containing SQDG species which accumulate in Arabidopsis leaf tissue during the HR triggered by recognition of AvrRpm1.

4. Experimental

4.1. Plant material and lipid extraction.

Arabidopsis thaliana were cultivated under short day conditions in a climate chamber as described (Kourtchenko et al., 2007). The dexamethasone inducible lines AvrRpm1:Col-0 and AvrRpm1:*rpm1-3* lines are also described elsewhere (Andersson et al., 2006b; Mackey et al., 2002). The DEX inducible AvrRpm1 construct was crossed into the *dde2-2* mutant (von Malek et al., 2002). A F₂-population was screened for male sterility (conferred by the *dde2-2* mutation) and sterile plants were rescued by

application of methyl jasmonate. F₃-seeds selected in this way were screened for complete penetrance of the DEX inducible HR phenotype. Leaf discs were punched out from leaves of 6-8 weeks old plants and placed in 20 µM dexamethasone (DEX, Sigma-Aldrich) in water and a total lipid extract was obtained as previously described (Andersson et al., 2006b). Briefly, 4 discs were incubated in boiling isopropanol for 5 min, dried under a flow of nitrogen and extracted in 1 ml of chloroform:methanol:water (1:2:0.8, by vol.) supplemented with 0.05% butylated hydroxytoluene (BHT) in a bath type sonicator for 30 min followed by 30 min in cold room. Phase separation was induced by addition of 0.25 ml of chloroform and 0.25 ml of 1.6 M HCl. The lipids were recovered from the lower phase and the aqueous phase re-extracted with 0.5 ml of chloroform.

4.2. Lipid analysis.

The total lipid extract was dried under N₂ and dissolved in a small volume of methanol and used directly for LC-MS. Alternatively, the dried extract was dissolved in chloroform and fractionated on a 100 mg silica SPE column (Supelco). Neutral lipids were eluted in chloroform, glycolipids in acetone and the phospholipids in methanol. The phospholipids were dried under nitrogen and dissolved in a small volume of methanol prior to LC-MS.

An Agilent 1260 HPLC system coupled to an Agilent 6410 triple quadrupole detector equipped with an electrospray interface was used for lipid analysis. The lipids were separated on an RP-MS Accucore 150x2.1 mm, 2.6 µm column (Thermo Scientific) thermostated to 50°C using a gradient from methanol:acetonitrile:water (35:35:30, by vol., A) to 2-propanol (B) at a constant flow of 0.25 ml*min⁻¹. Both solvents were supplemented with 0.2% formic acid, 0.1% ammonia and 5 µM H₃PO₄. A 5 min isocratic elution (100% A) was followed by a linear increase of B to 95% in 25 min followed by 5 min isocratic elution, reversal and re-equilibration of the column. The ion source was operated at 250°C and 4500 V with a nitrogen gas flow of 11 L*min⁻¹ at 40 psi.

LC-MS data were analyzed in Agilent Masshunter software. For profiling experiments the data files were converted to mzXML format using the MSconvert tool of the ProteoWizard package (Kessner et al., 2008) and further analyzed in MZmine 2.10. (Pluskal et al., 2010). Settings for peak discovery were manually adjusted until a satisfactory coverage of peaks was obtained. The combined aligned peak lists from MZmine 2.10 were exported and further analyzed in Microsoft Excel 2010. Correspondence analysis using the PAST software package (<http://folk.uio.no/ohammer/past>, version 2.14) was used in order to create a two-dimensional ordination of the samples.

4.3. Lipid purification and characterization of acylated OPDA-containing PG species.

A total lipid extract was obtained as described (Kourtchenko et al., 2007) from 100 g of DEX:AvrRpm1/Col-0 leaves incubated for four hours in dexamethasone solution (Andersson et al., 2006b). The total lipids were fractionated on a 6 g silica column (Si-60, Merck, Darmstadt, Germany). The acylated PG-species were eluted in chloroform:methanol (9:1, by vol) after washing in acetone and further purified by TLC (Si-60, Merck, Darmstadt, Germany) using the solvent system chloroform:methanol:NaOH (25%) (40:10:1, by vol.). The plate was scraped into 1 cm sections and lipids extracted in methanol from each fraction. The fractions were analyzed by LC-MS as described above for the RT m/z pairs corresponding to B1 and B2 in table 2. Both lipids were found in the fraction corresponding to Rf 0.5-0.6. This was further fractionated by HPLC using the same gradient as described above, except a 4.6x150 mm C18 Chromasil (HiChrom, Reading UK) column was used with a flow of 0.8 ml*min⁻¹ and a splitter installed post column. Approximately 85% of the total flow was diverted from the mass detector and fractions collected manually. GC-MS on transesterified lipids were as previously described (Nilsson et al., 2012). For accurate mass measurement, the purified lipids were dissolved in a mix of the mobile phases A and B (1:1, by vol.) and injected directly into the source of an Agilent 6510 QTOF mass spectrometer and analyzed in negative mode using the reference m/z 966.000725 (HP-0921 + formate) and 1033.988109 (HP-0921).

Acknowledgments

We thank Dr. Gunnar Cervin and the Marine Ecology research group at Tjärnö marine biological research laboratory for advice with accurate mass measurements and access to the qTOF instrument. The financial support of the Swedish Council for Environment, Agricultural Sciences and Spatial Planning (project no. 2007-1563, 2009-888 and 2007-1051) and the Olle Engkvist Byggmästare foundation is gratefully acknowledged.

Literature cited

- Adlercreutz, D., Wehtje, E., 2001. A simple HPLC method for the simultaneous analysis of phosphatidylcholine and its partial hydrolysis products 1- and 2-acyl lysophosphatidylcholine. *J Amer Oil Chem Soc* 78, 1007-1011.
- Andersson, M. X., Hamberg, M., Kourtchenko, O., Brunnström, Å., McPhail, K. L., Gerwick, W. H., Göbel, C., Feussner, I., Ellerstrom, M., 2006a. Oxylinin Profiling of the Hypersensitive Response in *Arabidopsis thaliana*: Formation of a Novel Oxo-phytodienoic Acid-containing Galactolipid, *Arabidopsis* E. J. Biol. Chem. 281, 31528-31537.
- Andersson, M. X., Kourtchenko, O., Dangl, J. L., Mackey, D., Ellerström, M., 2006b. Phospholipase dependent signalling during the AvrRpm1- and AvrRpt2-induced disease resistance responses in *Arabidopsis thaliana*. *Plant J.* 47, 947-959.

Andreou, A., Brodhun, F., Feussner, I., 2009. Biosynthesis of oxylipins in non-mammals. *Prog. Lipid Res.* 48, 148-170.

Bent, A. F., Mackey, D., 2007. Elicitors, Effectors, and R Genes: The New Paradigm and a Lifetime Supply of Questions. *Annual Review of Phytopathology* 45, 399-436.

Browse, J., 2009. Jasmonate passes muster: A receptor and targets for the defense hormone. *Annu. Rev. Plant Biol.* 60, 183-205.

Brügger, B., Erben, G., Sandhoff, R., Wieland, F. T., Lehmann, W. D., 1997. Quantitative analysis of biological membrane lipids at the low picomole level by nano-electrospray ionization tandem mass spectrometry. *Proceedings of the National Academy of Sciences* 94, 2339-2344.

Buseman, C. M., Tamura, P., Sparks, A. A., Baughman, E. J., Maatta, S., Zhao, J., Roth, M. R., Esch, S. W., Shah, J., Williams, T. D., Welti, R., 2006. Wounding stimulates the accumulation of glycerolipids containing oxophytodienoic acid and dinor-oxophytodienoic acid in *Arabidopsis* leaves. *Plant Physiol.* 142, 28-39.

Cole, M. J., Enke, C. G., 1991. Fast-Atom-Bombardment Tandem Mass-Spectrometry Employing Ion-Molecule Reactions for the Differentiation of Phospholipid Classes. *J Am Soc Mass Spectr* 2, 470-475.

Creer, M. H., Gross, R. W., 1985. Separation of isomeric lysophospholipids by reverse phase HPLC. *Lipids* 20, 922-928.

Dorne, A. J., Heinz, E., 1989. Position and pairing of fatty acids in phosphatidylglycerol from pea leaf chloroplasts and mitochondria. *Plant Sci.* 60, 39-46.

Fauconnier, M.-L., Williams, T. D., Marlier, M., Welti, R., 2003. Potato tuber phospholipids contain colneleic acid in the 2-position. *FEBS Lett.* 538, 155-158.

Gage, D. A., Huang, Z. H., Benning, C., 1992. Comparison of sulfoquinovosyl diacylglycerol from spinach and the purple bacterium *Rhodobacter spaeroides* by fast atom bombardment tandem mass spectrometry. *Lipids* 27, 632-636.

Gfeller, A., Liechti, R., Farmer, E. E., 2010. *Arabidopsis* jasmonate signaling pathway. *Science Signaling* 3.

Glauser, G., Dubugnon, L., Mousavi, S. A. R., Rudaz, S., Wolfender, J. L., Farmer, E. E., 2009. Velocity Estimates for Signal Propagation Leading to Systemic Jasmonic Acid Accumulation in Wounded *Arabidopsis*. *J. Biol. Chem.* 284, 34506-34513.

Grant, M. R., Godiard, L., Straube, E., Ashfield, T., Lewald, J., Sattler, A., Innes, R. W., Dangl, J. L., 1995. Structure of the *Arabidopsis* RPM1 gene enabling dual specificity disease resistance. *Science* 269, 843-846.

Hisamatsu, Y., Goto, N., Hasegawa, K., Shigemori, H., 2003. Arabidopsides A and B, two new oxylipins from *Arabidopsis thaliana*. *Tetrahedron Lett.* 44, 5553-5556.

Hisamatsu, Y., Goto, N., Sekiguchi, M., Hasegawa, K., Shigemori, H., 2005. Oxylipins arabidopsides C and D from *Arabidopsis thaliana*. *J. Nat. Prod.* 68, 600-603.

Holmback, J., Karlsson, A. A., Arnoldsson, K. C., 2001. Characterization of N-acylphosphatidylethanolamine and acylphosphatidylglycerol in oats. *Lipids* 36, 153-165.

Ibrahim, A., Schutz, A. L., Galano, J. M., Herrfurth, C., Feussner, K., Durand, T., Brodhun, F., Feussner, I., 2011. The Alphabet of Galactolipids in *Arabidopsis thaliana*. *Frontiers in plant science* 2, 95.

Isaac, G., Jeannotte, R., Esch, S., Welti, R., 2007. New Mass-Spectrometry-Based Strategies For Lipids. In: Setlow, J. (Ed.), *Genetic Engineering*, vol. 28. Springer US, pp. 129-157.

Jones, J. D. G., Dangl, J. L., 2006. The plant immune system. *Nature* 444, 323-329.

Kessner, D., Chambers, M., Burke, R., Agus, D., Mallick, P., 2008. ProteoWizard: open source software for rapid proteomics tools development. *Bioinformatics* 24, 2534-2536.

Kirik, A., Mudgett, M. B., 2009. SOBER1 phospholipase activity suppresses phosphatidic acid accumulation and plant immunity in response to bacterial effector AvrBsT. *Proceedings of the National Academy of Sciences* 106, 20532-20537.

Kourtchenko, O., Andersson, M. X., Hamberg, M., Brunnstrom, A., Gobel, C., McPhail, K. L., Gerwick, W. H., Feussner, I., Ellerstrom, M., 2007. Oxo-phytodienoic acid-containing galactolipids in *Arabidopsis*: Jasmonate signaling dependence. *Plant Physiol.* 145, 1658-1669.

Laaksonen, R., Katajamaa, M., Paiva, H., Sysi-Aho, M., Saarinen, L., Junni, P., Lutjohann, D., Smet, J., Van Coster, R., Seppanen-Laakso, T., Lehtimaki, T., Soini, J., Oresic, M., 2006. A systems biology strategy reveals biological pathways and plasma biomarker candidates for potentially toxic statin-induced changes in muscle. *PLoS one* 1, e97.

Li-Beisson, Y., Shorrosh, B., Beisson, F., Andersson, M. X., Arondel, V., Bates, P. D., Baud, S., Bird, D., Debono, A., Durrett, T. P., Franke, R. B., Graham, I. A., Katayama, K., Kelly, A. A., Larson, T., Markham, J. E., Miquel, M., Molina, I., Nishida, I., Rowland, O., Samuels, L., Schmid, K. M., Wada, H., Welti, R., Xu, C., Zallot, R., Ohlrogge, J., 2010. Acyl-lipid metabolism. *The Arabidopsis book / American Society of Plant Biologists* 8, e0133.

Li, M., Hong, Y., Wang, X., 2009. Phospholipase D- and phosphatidic acid-mediated signaling in plants. *Biochim Biophys Acta* 1791, 927-935.

Mackey, D., Holt, B. F., Wiig, A., Dangl, J. L., 2002. RIN4 Interacts with *Pseudomonas syringae* Type III Effector Molecules and Is Required for RPM1-Mediated Resistance in *Arabidopsis*. *Cell* 108, 743-754.

Monaghan, J., Zipfel, C., 2012. Plant pattern recognition receptor complexes at the plasma membrane. *Current opinion in plant biology* 15, 349-357.

Montillet, J. L., Chamnongpol, S., Rusterucci, C., Dat, J., van de Cotte, B., Agnel, J. P., Battesti, C., Inze, D., Van Breusegem, F., Triantaphylides, C., 2005. Fatty acid hydroperoxides and H₂O₂ in the execution of hypersensitive cell death in tobacco leaves. *Plant Physiol.* 138, 1516-1526.

Moreau, P., Bessoule, J. J., Mongrand, S., Testet, E., Vincent, P., Cassagne, C., 1998. Lipid trafficking in plant cells. *Prog. Lipid Res.* 37, 371-391.

Nilsson, A. K., Fahlberg, P., Ellerstrom, M., Andersson, M. X., 2012. Oxo-phytodienoic acid (OPDA) is formed on fatty acids esterified to galactolipids after tissue disruption in *Arabidopsis thaliana*. *FEBS Lett.* 586, 2483-2487.

Ogiso, H., Suzuki, T., Taguchi, R., 2008. Development of a reverse-phase liquid chromatography electrospray ionization mass spectrometry method for lipidomics, improving detection of phosphatidic acid and phosphatidylserine. *Anal Biochem* 375, 124-131.

Okazaki, Y., Kamide, Y., Hirai, M. Y., Saito, K., 2013. Plant lipidomics based on hydrophilic interaction chromatography coupled to ion trap time-of-flight mass spectrometry. *Metabolomics : Official journal of the Metabolomic Society* 9, 121-131.

Pinosa, F., Buhot, N., Kwaaitaal, M., Fahlberg, P., Thordal-Christensen, H., Ellerstrom, M., Andersson, M. X., 2013. *Arabidopsis* phospholipase Ddelta is involved in basal defense and non-host resistance to powdery mildew fungi. *Plant Physiol.*

Pluskal, T., Castillo, S., Villar-Briones, A., Oresic, M., 2010. MZmine 2: Modular framework for processing, visualizing, and analyzing mass spectrometry-based molecular profile data. *BMC Bioinformatics* 11.

Retra, K., Bleijerveld, O. B., van Gestel, R. A., Tielens, A. G., van Hellemond, J. J., Brouwers, J. F., 2008. A simple and universal method for the separation and identification of phospholipid molecular species. *Rapid communications in mass spectrometry : RCM* 22, 1853-1862.

Rusterucci, C., Montillet, J.-L., Agnel, J.-P., Battesti, C., Alonso, B., Knoll, A., Bessoule, J.-J., Etienne, P., Suty, L., Blein, J.-P., Triantaphylides, C., 1999. Involvement of Lipoxygenase-dependent Production of Fatty Acid Hydroperoxides in the Development of the Hypersensitive Cell Death induced by Cryptogein on Tobacco Leaves. *J. Biol. Chem.* 274, 36446-36455.

Samarakoon, T., Shiva, S., Lowe, K., Tamura, P., Roth, M. R., Welti, R., 2012. *Arabidopsis thaliana* membrane lipid molecular species and their mass spectral analysis. *Methods Mol Biol* 918, 179-268.

Sato, M., Tsuda, K., Wang, L., Collier, J., Watanabe, Y., Glazebrook, J., Katagiri, F., 2010. Network modeling reveals prevalent negative regulatory relationships between signaling sectors in *Arabidopsis* immune signaling. *PLoS pathogens* 6, e1001011.

Schaller, A., Stintzi, A., 2009. Enzymes in jasmonate biosynthesis - Structure, function, regulation. *Phytochemistry* 70, 1532-1538.

Taguchi, R., Houjou, T., Nakanishi, H., Yamazaki, T., Ishida, M., Imagawa, M., Shimizu, T., 2005. Focused lipidomics by tandem mass spectrometry. *Journal of chromatography. B, Analytical technologies in the biomedical and life sciences* 823, 26-36.

Testerink, C., Munnik, T., 2011. Molecular, cellular, and physiological responses to phosphatidic acid formation in plants. *J Exp Bot* 62, 2349-2361.

Tsuda, K., Sato, M., Stoddard, T., Glazebrook, J., Katagiri, F., 2009. Network properties of robust immunity in plants. *PLoS genetics* 5, e1000772.

van der Luit, A. H., Piatti, T., van Doorn, A., Musgrave, A., Felix, G., Boller, T., Munnik, T., 2000. Elicitation of Suspension-Cultured Tomato Cells Triggers the Formation of Phosphatidic Acid and Diacylglycerol Pyrophosphate. *Plant Physiol* 123, 1507-1516.

Wang, X., 2004. Lipid signaling. *Current opinion in plant biology* 7, 329-336.

Welti, R., Li, W. Q., Li, M. Y., Sang, Y. M., Biesiada, H., Zhou, H. E., Rajashekar, C. B., Williams, T. D., Wang, X. M., 2002. Profiling membrane lipids in plant stress responses - Role of phospholipase D alpha in freezing-induced lipid changes in Arabidopsis. *J. Biol. Chem.* 277, 31994-32002.

Welti, R., Wang, X., Williams, T. D., 2003. Electrospray ionization tandem mass spectrometry scan modes for plant chloroplast lipids. *Analytical Biochemistry* 314, 149-152.

von Malek, B., van der Graaff, E., Schneitz, K., Keller, B., 2002. The Arabidopsis male-sterile mutant *dde2-2* is defective in the ALLENE OXIDE SYNTHASE gene encoding one of the key enzymes of the jasmonic acid biosynthesis pathway. *Planta* 216, 187-192.

Vu, H. S., Tamura, P., Galeva, N. A., Chaturvedi, R., Roth, M. R., Williams, T. D., Wang, X. M., Shah, J., Welti, R., 2012. Direct infusion mass spectrometry of oxylipin-containing arabidopsis membrane lipids reveals varied patterns in different stress responses. *Plant Physiol.* 158, 324-339.

Zhao, J., Devaiah, S. P., Wang, C., Li, M., Welti, R., Wang, X., 2013. Arabidopsis phospholipase Dbeta1 modulates defense responses to bacterial and fungal pathogens. *The New phytologist* 199, 228-240.

Zoeller, M., Stingl, N., Krischke, M., Fekete, A., Waller, F., Berger, S., Mueller, M. J., 2012. Lipid Profiling of the Arabidopsis Hypersensitive Response Reveals Specific Lipid Peroxidation and Fragmentation Processes: Biogenesis of Pimelic and Azelaic Acid. *Plant Physiol.* 160, 365-378.

Tables

Table 1. Fragmentation modes used for different lipid classes

Head group specific fragmentations of phospho- and galactolipids reported in the literature, used in this study for construction of species specific MRMs as listed in table S1.

Lipid class	Adduct	Transition type	Transition (<i>m/z</i>)
MGDG (“normal” fatty acids and OPDA containing)	NH ₄ ⁺	Neutral loss	179 ¹
DGDG (“normal” fatty acids and OPDA containing)	NH ₄ ⁺	Neutral loss	341 ¹
SQDG	-H	Precursor	225 ²
PC and lyso-PC	H ⁺	Precursor	184 ³
PE	H ⁺	Neutral loss	141 ³
PG	NH ₄ ⁺	Neutral loss	189 ⁴
PA	NH ₄ ⁺	Neutral loss	115 ⁵
PI	H ⁺	Neutral loss	260 ⁶
Acylated MGDG species	NH ₄ ⁺	Neutral loss	179 + acyl group ⁷

¹(Isaac et al., 2007), ²(Gage et al., 1992; Welti et al., 2003), ³(Brügger et al., 1997), ⁴(Taguchi et al., 2005), ⁵(Li-Beisson et al., 2010), ⁶(Cole and Enke, 1991), ⁷(Ibrahim et al., 2011)

Table 2. Phospholipid species induced by recognition of AvrRpm1 identification

Leaf discs from DEX:AvrRpm1/Col-0, DEX:AvrRpm1/*rpm1-3* and DEX:AvrRpm1/*dde2-2* were incubated in DEX solution for 0 or 6 hours and a phospholipid fraction was obtained. The phospholipids were separated on LC-MS using scanning from 400-1200 *m/z*. Peaks were identified using automated peak detection in MZmine 2. Peaks induced significantly (Student’s t-test, *p*<0.05) more than three-fold in DEX:AvrRpm1/Col-0 compared to DEX:AvrRpm1/*rpm1-3* were filtered out.

Finally these were sorted as dependent on AOS (more than three-fold larger peak area in DEX:AvrRpm1/Col-0 than in DEX:AvrRpm1/*dde2-2,7-14*) or independence of AOS (1-6).

Compound ID	m/z	Retention time (min)	Peak area ratio, Col-0 6 h / <i>rpm1-3</i> 6 h	Peak area ratio Col-0 6 h / <i>dde2-2</i> 6 h
2	847.5	19.4	14.2	1.0
2	879.5	16.3	6.8	0.3
3	883.5	17.8	4.5	0.7
4	861.5	18.3	4.4	0.7
5	881.4	17.3	3.1	0.5
6	693.4	21.9	3.0	0.8
7	1029.7	20.4	25.8	270.5
8	1031.6	20.6	25.7	282.1
9	755.4	17.8	51.4	173.5
10	757.5	18.4	20.9	12.1
11	855.4	18.4	10.2	136.2
12	845.4	18.3	8.6	78.2
13	865.4	8.2	23.6	108.6
14	829.5	18.2	5.2	343.3

Table 3. Identification of phospholipids induced by recognition of AvrRpm1

Product ion spectra in negative and positive mode were collected during chromatography of a phospholipid fraction obtained from DEX:AvrRpm1/Col-0 material at 6 hpi to identify compounds 1, 6 and 7-14 in table 1. Fractions containing the respective peaks were collected and accurate masses determined by direct infusion into the electrospray source of a QTOF spectrometer. n.d. not determined.

Compound ID	m/z	Fragments used for identification (negative mode)	Fragments used for identification (positive mode)	Interpretation (Fatty acids-headgroup)	Theoretical m/z of [-H]	Measured exact m/z negative mode QTOF
1	847.5	255.2 293.2	589.4	16:0,18:3- OH-PI ¹	847.4973	847.4974

		241.0				
6	693.4	279.2	n.d.	18:2, 18:3- PA ²	694.4576	n.d.
		277.2				
7	1029.7	253.2	585.5	16:1, OPDA- PG-OPDA	1029.6432	1029.6431
		291.2				
8	1031.6	255.2	587.5	16:0, OPDA- PG-OPDA	1031.6589	1031.6592
		291.2				
9	755.4	253.3	585.5	16:1, OPDA- PG ³	755.4499	755.4499
		291.2				
10	757.5	255.2	587.5	16:0, OPDA- PG ³	757.4656	757.4662
		291.2				
11	855.4	291.2	n.d.	18:4-O, 18:1- SQDG	855.4928	855.4931
		281.2				
		225.0				
12	845.4	255.2	587.5	18:4-O, 16:0- PI	845.4816	845.4819
		291.2				
		241.0				
13	865.4	291.2	n.d.	OPDA, OPDA-SQDG	865.4408	865.4410
		225.0				
14	829.5	255.1	n.d.	16:0, OPDA- SQDG	829.4772	829.4773
		291.3				
		225.0				

¹Described by (Zoeller et al., 2012)

²Verified by authentic standard chromatographed under identical conditions

³Described by (Buseman et al., 2006)

Figure legends

Fig. 1 *Development of an LC-MS method for profiling Arabidopsis glycerolipids*

A total lipid extract obtained from Arabidopsis leaf tissue was analyzed by reverse phase LC-MS/MS using the head and diacyl-group specific MRMs defined in table 1 and detailed in table S1. The lipid classes were analyzed in two separate runs, one in positive mode for PC (A), PE (B), PG (C), PA (D), lyso-PC (E), MGDG (F), DGDG (G), OPDA-containing MGDG (I) and acylated MGDG species (J), and one in negative mode for SQDG (H). Annotation shows apparent number of carbons, double bonds and “extra” oxygens in each lipid species. In I and J the one letter designation of arabidopsides is used. For the acylated MGDG species (H) the apparent carbon and double bond number of the diacylglycerol group is annotated along with the fatty acid bound to the head group.

Fig. 2 *Ion leakage triggered by recognition of AvrRpm1 is independent of functional AOS*

Leaf discs were punched out from leaves of the three indicated Arabidopsis lines and floated on water. After addition of the chemical inducer DEX, the conductivity of the bathing solution was measured at the indicated time points (A). Average and 95% confidence interval of six replicates are shown. B. Leaf discs treated in the same way were taken out of the solution at the indicated time points, blotted against Kleenex and weighed immediately or after drying at 60°C for three days. Average and range of duplicate samples is shown.

Fig. 3 *Separation of Arabidopsis leaf phospholipids in negative full scan mode and statistical description of the phospholipid profile*

A phospholipid fraction obtained from Arabidopsis wild type leaf tissue was separated by reverse phase LC and the lipids detected by electrospray MS in full scan. The data was exported to MZmine2 and plotted in 2D as m/z against retention time (A). Aligned data for two replicate samples of the three indicated lines at zero time and 6 hours after induction of AvrRpm1 transcription with DEX addition were analyzed for statistical correlation using correspondence analysis in PAST (B).

Fig. 4 *Quantification of phospholipids induced independently or depending on AOS in the HR*

Lipid fractions were obtained from DEX:AvrRpm1/Col-0, DEX:AvrRpm1/*dde2-2* and DEX:AvrRpm1/*rpm1-3* incubated in dexamethasone solution for the indicated time points and analyzed by LC-MS in single ion monitoring mode. Peak areas were normalized to DEX:AvrRpm1/Col-0 zero time for all lipids. Average and range of duplicate samples are shown. A. Peaks induced independently of AOS. B. Peaks induced in an AOS-dependent manner.

Fig. 5 *Quantification of glycerolipids in the hypersensitive response*

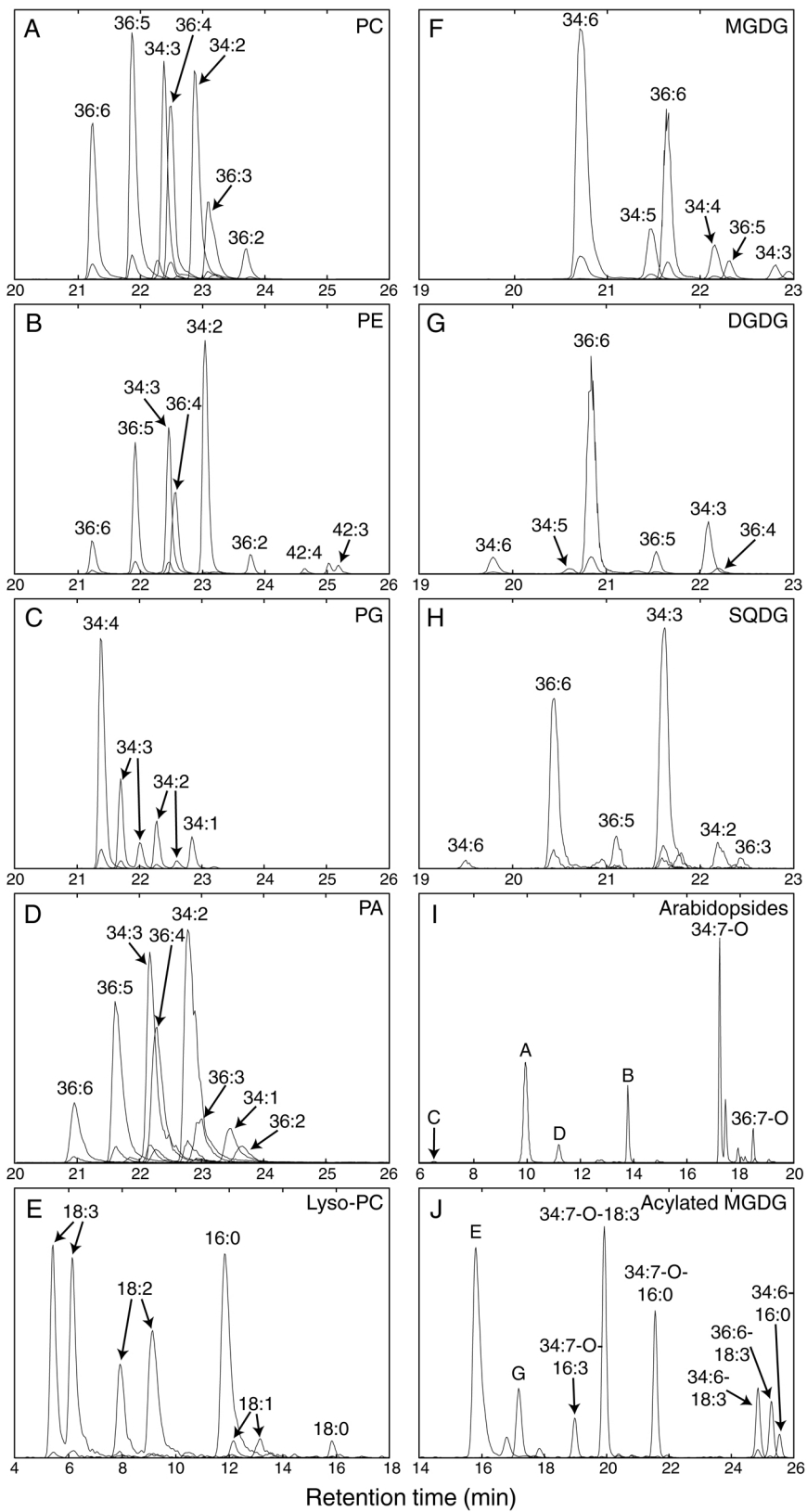
Lipid fractions were obtained from DEX:AvrRpm1/Col-0, DEX:AvrRpm1/*dde2-2* and DEX:AvrRpm1/*rpm1-3* incubated in dexamethasone solution for the indicated time points and analyzed by LC-MS/MS in MRM mode using the MRMs listed in table S1. Peak areas were normalized to DEX:AvrRpm1/Col-0 zero time for all lipids. Diacyl glycerolipids are shown in **A** and acylated galactolipids in **B**. Average and range of duplicate samples are shown.

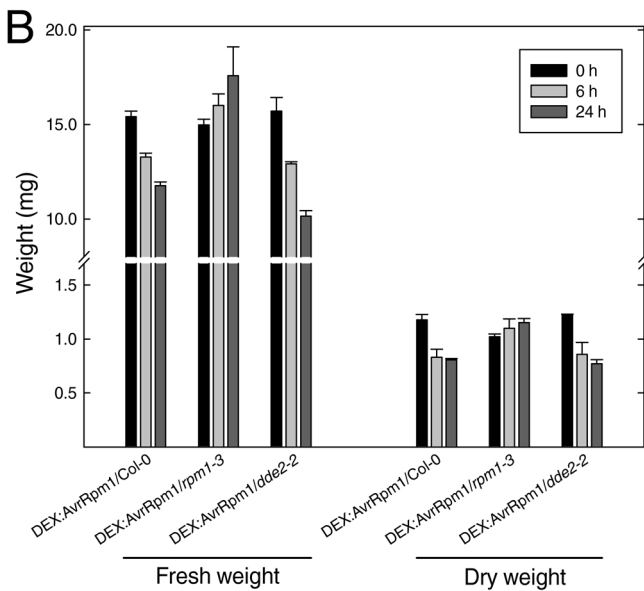
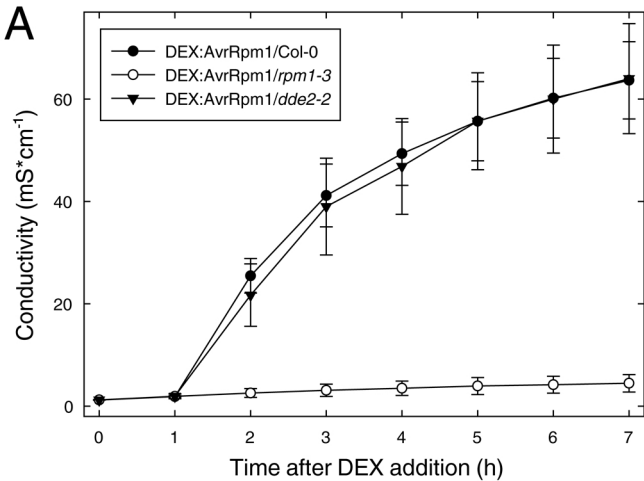
Fig. 6 *Putative structure of acylated OPDA containing PG species*

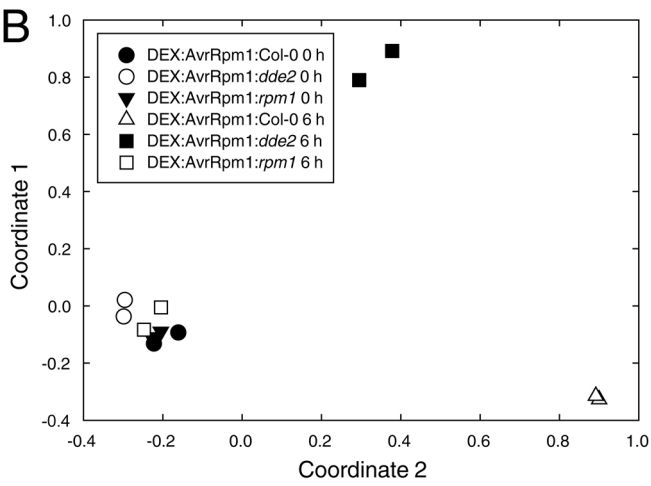
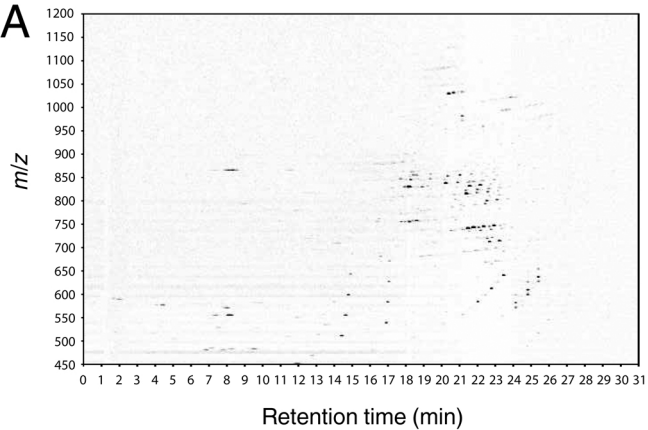
The putative structures are based on acyl fragments, GC-MS separation of fatty acid methyl esters and total mass as determined by electrospray time of flight MS. The data presented herein cannot strictly assign which hydroxyl groups on the backbone and the headgroup binds OPDA. However, the known structure of thylakoid PG species and acylated PG isolated from oat seeds support the presented structure.

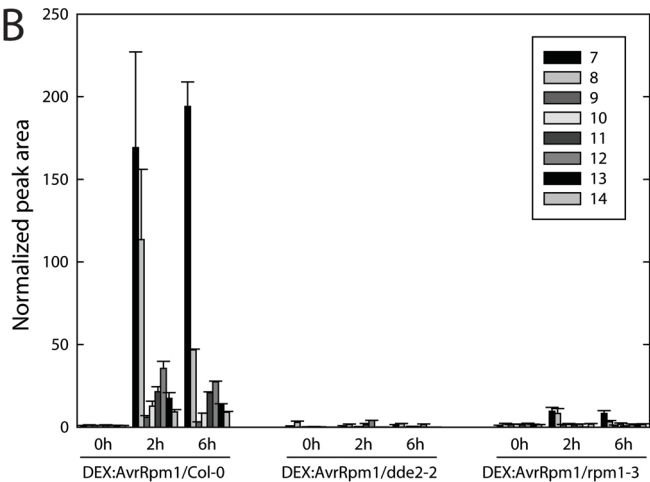
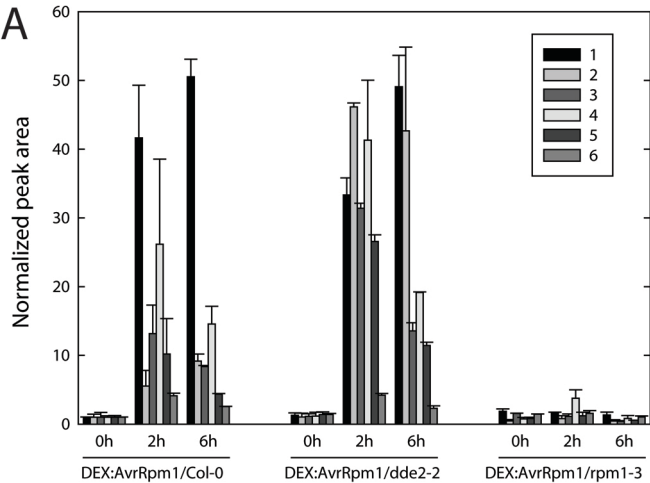
Fig. 7 *Analysis of PI species during the HR*

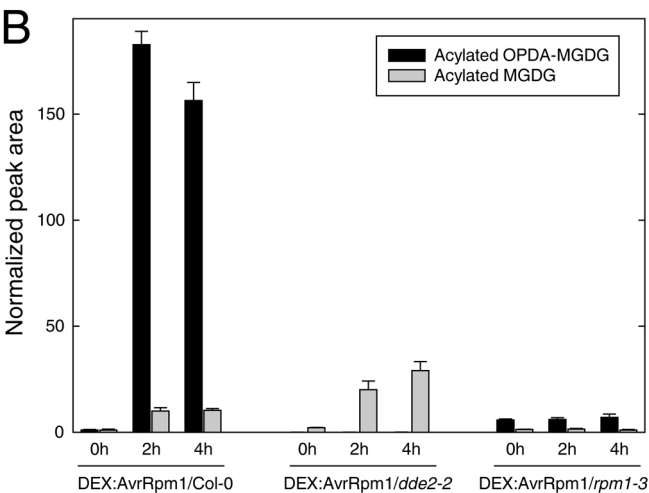
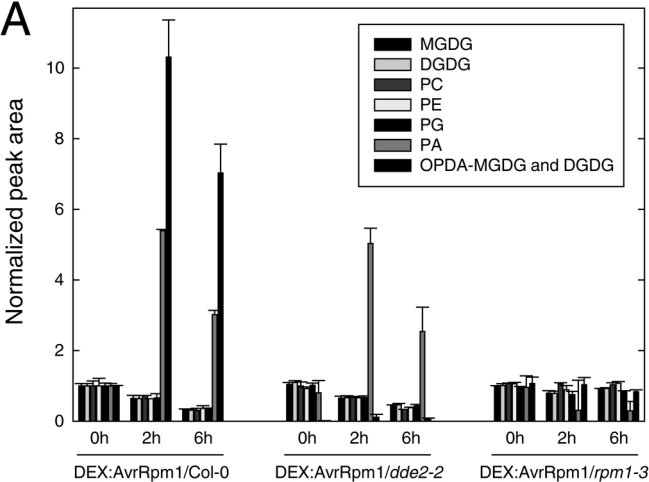
Lipid fractions were obtained from DEX:AvrRpm1/Col-0, DEX:AvrRpm1/*rpm1-3* and DEX:AvrRpm1/*dde2-2* and subjected to LC-MS/MS using neutral loss of m/z 260 as a head group specific scan for PI-species. **A**. Total ion chromatogram is shown for DEX:AvrRpm1/Col-0 at zero time and 6 hours after induction of AvrRpm1 transcription. **B**. Quantification of the three indicated PI-species in the three lines at 0, 2 and 6 hours after induction of AvrRpm1 transcription. Average and range of two replicates are shown.

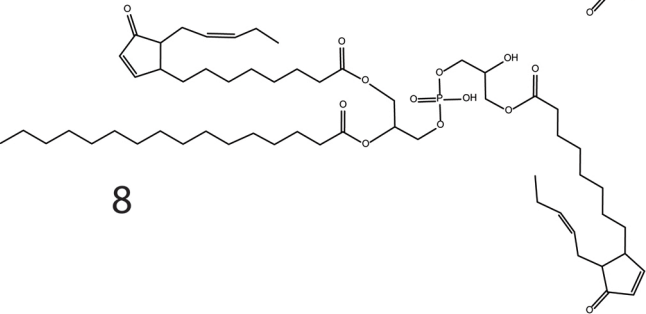
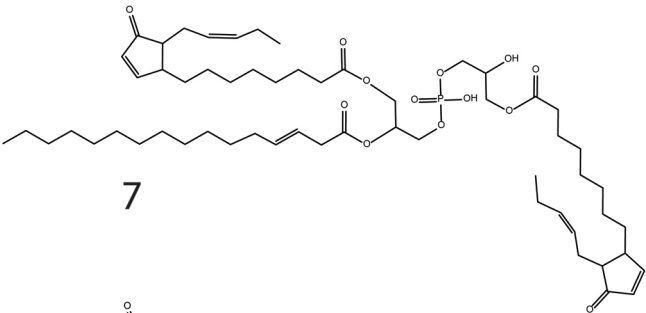












A

Detector response

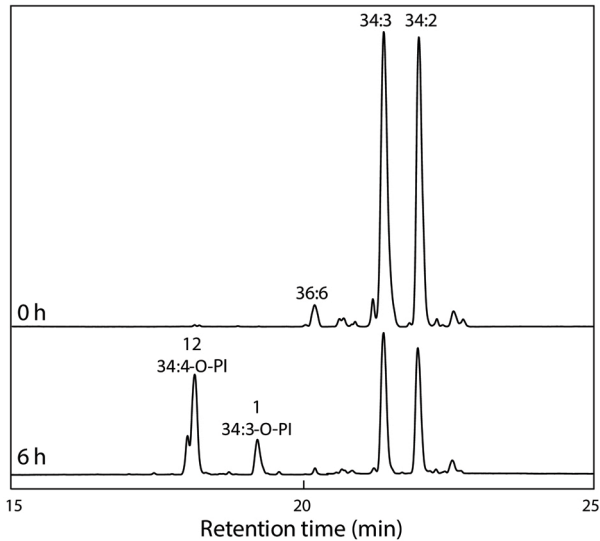
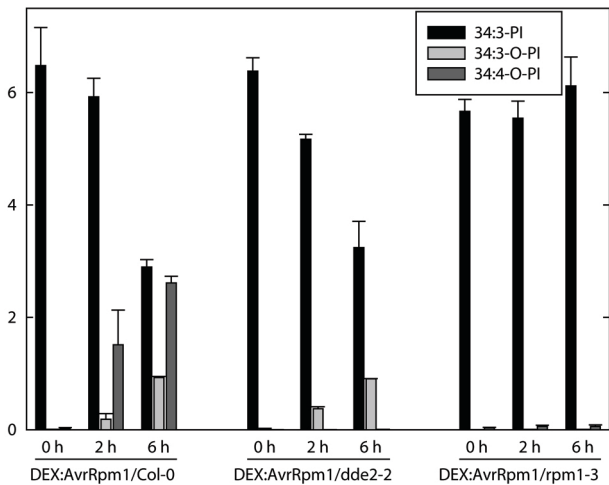
**B**Peak area (counts*10⁵)

Table S1. Arabidopsis lipid species analyzed

Specific MRMs were designed for major Arabidopsis leaf glycerolipid species according to (Ibrahim et al., 2011; Isaac et al., 2007; Samarakoon et al., 2012).

No.	Lipid species (DAG total C:double bonds-extra oxygen-headgroup)	Monoisotopic weight	Adduct and polarity	Precursor	Product
1	34:6-MGDG	746.6	NH ₄ ⁺	764.6	585.5
2	34:5-MGDG	748.6	NH ₄ ⁺	766.6	587.5
3	34:4-MGDG	750.6	NH ₄ ⁺	768.7	589.6
4	34:3-MGDG	752.6	NH ₄ ⁺	770.7	591.6
4	34:2-MGDG	754.7	NH ₄ ⁺	772.7	593.6
6	36:6-MGDG	774.6	NH ₄ ⁺	792.7	613.6
7	36:5-MGDG	776.6	NH ₄ ⁺	794.7	615.6
8	36:4-MGDG	778.7	NH ₄ ⁺	796.7	617.6
9	36:3-MGDG	780.7	NH ₄ ⁺	798.7	619.6
10	34:6-DGDG	908.7	NH ₄ ⁺	926.8	585.3
11	34:5-DGDG	910.7	NH ₄ ⁺	928.8	587.3
12	34:4-DGDG	912.8	NH ₄ ⁺	930.8	589.3
13	34:3-DGDG	914.8	NH ₄ ⁺	932.8	591.3
14	36:6-DGDG	936.8	NH ₄ ⁺	954.8	613.3
15	36:5-DGDG	938.8	NH ₄ ⁺	956.8	615.3
16	36:4-DGDG	940.8	NH ₄ ⁺	958.8	617.3
17	34:6-SQDG	810.6	-H	809.5	225.0
18	34:4-SQDG	814.6	-H	813.6	225.0
19	34:3-SQDG	816.6	-H	815.6	225.0
20	34:2-SQDG	818.6	-H	817.6	225.0
21	36:6-SQDG	838.6	-H	837.6	225.0
22	36:5-SQDG	840.6	-H	839.6	225.0
23	36:4-SQDG	842.6	-H	841.6	225.0
24	36:3-SQDG	844.6	-H	843.6	225.0

25	34:2-PC	757.6	H ⁺	758.6	184.1
26	34:3-PC	755.5	H ⁺	756.6	184.1
27	36:2-PC	785.6	H ⁺	786.6	184.1
28	36:3-PC	783.6	H ⁺	784.6	184.1
29	36:4-PC	781.6	H ⁺	782.6	184.1
30	36:5-PC	779.5	H ⁺	780.6	184.1
31	36:6-PC	777.5	H ⁺	778.5	184.1
32	16:0-lysoPC	495.3	H ⁺	496.3	184.1
33	18:0-lysoPC	523.4	H ⁺	524.4	184.1
34	18:1-lysoPC	521.3	H ⁺	522.4	184.1
35	18:2-lysoPC	519.3	H ⁺	520.3	184.1
36	18:3-lysoPC	517.3	H ⁺	518.3	184.1
37	34:2-PE	715.5	H ⁺	716.5	575.5
38	34:3-PE	713.5	H ⁺	714.5	573.5
39	36:2-PE	743.5	H ⁺	744.6	603.6
40	36:3-PE	741.5	H ⁺	742.5	601.5
41	36:4-PE	739.5	H ⁺	740.5	599.5
42	36:5-PE	737.5	H ⁺	738.5	597.5
43	36:6-PE	735.5	H ⁺	736.5	595.5
44	42:4-PE	823.6	H ⁺	824.6	683.6
45	42:3-PE	825.6	H ⁺	826.6	685.6
46	34:1-PA	674.5	NH ₄ ⁺	692.5	577.4
47	34:2-PA	672.5	NH ₄ ⁺	690.5	575.4
48	34:3-PA	670.5	NH ₄ ⁺	688.5	573.4
49	36:2-PA	700.5	NH ₄ ⁺	718.5	603.4
50	36:3-PA	698.5	NH ₄ ⁺	716.5	601.4
51	36:4-PA	696.5	NH ₄ ⁺	714.5	599.4
52	36:5-PA	694.5	NH ₄ ⁺	712.5	597.4
53	36:6-PA	692.4	NH ₄ ⁺	710.5	595.4
54	34:1-PG	748.5	NH ₄ ⁺	766.6	577.6

55	34:2-PG	746.5	NH ₄ ⁺	764.5	575.5
56	34:3-PG	744.5	NH ₄ ⁺	762.5	573.5
57	34:4-PG	742.5	NH ₄ ⁺	760.5	571.5
58	Arabidopside B	802.6	NH ₄ ⁺	820.6	641.5
59	Arabidopside A	774.5	NH ₄ ⁺	792.6	613.4
60	Arabidopside D	964.7	NH ₄ ⁺	982.8	641.5
61	Arabidopside C	936.7	NH ₄ ⁺	954.7	613.4
62	36:7-O-MGDG	788.6	NH ₄ ⁺	806.6	627.5
63	34:7-O-MGDG	760.6	NH ₄ ⁺	778.6	599.5
64	Arabidopside G	1076.8	NH ₄ ⁺	1094.8	641.5
65	Arabidopside E	1048.7	NH ₄ ⁺	1066.8	613.4
66	34:7-O-MGDG-18:3	1034.8	NH ₄ ⁺	1052.9	613.5
67	34:7-O-MGDG-16:3	1006.8	NH ₄ ⁺	1024.8	613.5
68	34:7-O-MGDG-16:0	1012.8	NH ₄ ⁺	1030.9	613.5
69	36:6-MGDG-18:3	1034.8	NH ₄ ⁺	1052.9	613.5
70	34:6-MGDG-16:0	984.8	NH ₄ ⁺	1002.9	585.5
71	34:6-MGDG-18:3	1006.8	NH ₄ ⁺	1024.8	585.5
72	36:6-MGDG-16:3	1006.8	NH ₄ ⁺	1024.8	613.5
